

Cite this: *Chem. Sci.*, 2024, 15, 18318

All publication charges for this article have been paid for by the Royal Society of Chemistry

Exploring efficient and air-stable d^2 Re(v) alkylidyne catalysts: toward room temperature alkyne metathesis †

Mingxu Cui, ^{‡a} Jie Huang, ^{‡a} Long Yiu Tsang, ^a Herman H. Y. Sung,^a Ian D. Williams ^{*a} and Guochen Jia ^{*ab}

Transition metal-catalyzed alkyne metathesis has become a useful tool in synthetic chemistry. Well-defined alkyne metathesis catalysts comprise alkylidyne complexes of tungsten, molybdenum and rhenium. Non- d^0 Re(v) alkylidyne catalysts exhibit advantages such as remarkable tolerance to air and moisture as well as excellent functional group compatibility. However, the known Re(v) alkylidynes with a pyridine leaving ligand require harsh conditions for activation, resulting in lower catalytic efficiency compared to d^0 Mo(vi) and W(vi) alkylidynes. Herein, we report the first non- d^0 alkylidyne complex capable of mediating alkyne metathesis at room temperature, namely, the Re(v) aqua alkylidyne complex $\text{Re}(\equiv\text{CCH}_2\text{Ph})(^i\text{PrPO})_2(\text{H}_2\text{O})$ (**14**). The aqua complex readily dissociates a water ligand in solution, confirmed by ligand substitution reactions with other σ -donor ligands. The aqua complex can be readily prepared on a large scale, and is stable to air and moisture in the solid state and compatible with a variety of functional groups. The versatile ability of the catalyst has been demonstrated through examples of alkyne cross-metathesis (ACM), ring-closing alkyne metathesis (RCAM), and acyclic diyne metathesis macrocyclization (ADIMAC) reactions. All in all, this work presents a solution for an efficient and air-stable alkyne metathesis catalytic system based on d^2 Re(v)-alkylidynes.

Received 10th August 2024

Accepted 2nd October 2024

DOI: 10.1039/d4sc05369a

rsc.li/chemical-science

Introduction

Transition metal-catalyzed alkyne metathesis has emerged as a highly valuable synthetic tool in constructing molecules with a C–C triple bond,¹ finding increasing applications in both organic synthesis² and material science.^{3–7} Highly efficient alkyne metathesis catalysts are usually 4-coordinate tetrahedral alkylidyne complexes of Mo(vi)^{8,9} and W(vi)¹⁰ supported by alkoxide, aryloxy, or silyloxy ligands (Chart 1, top). The low-coordinate and electron-deficient natures of these catalysts make them highly sensitive to moisture, requiring particularly vigorous techniques/conditions for handling and storage.

An ideal catalyst should possess three key characteristics:¹¹ (1) it can be easily prepared from cheap commercially available materials; (2) it should be active enough to effect catalytic reactions at ambient or slightly elevated temperatures in a reasonable time period; (3) it should be reasonably stable toward air & moisture and has high functional-group tolerance.

Recent advancements in alkyne metathesis catalyst development have shifted focus toward enhancing catalyst stability, crucial for enabling practical handling in synthetic labs without the need for strict air/moisture-free equipment.¹² Strategies include utilizing strong σ donating NHC ligands (e.g. **5**)¹³ or polydentate ligands (e.g. **6**,^{14–16} **7**^{17,18}) to stabilize low-coordinate and electron-deficient centers of Mo or W. Encapsulation of active species in paraffin wax provided an alternative way to extend their lifetime in air (**7**).¹⁷ Another strategy toward air-stable Mo alkylidynes involves associating N-based sigma-donors like pyridine and 1,9-phenanthroline with the 4-coordinated metal center to form 5- or 6-coordinated alkylidyne complexes (e.g. **8**).^{9,19} at the expense of lowering or losing activity. Activation of complex **8** is required (e.g. with a Lewis acid such as MnCl_2 or ZnCl_2 at 80 °C) prior to use. Achieving both high activity and stability simultaneously is challenging. A recent advancement is the invention of the pyridine-supported catalyst **9**, which closely aligns with these goals. With fine-tuning of a tripodal ligand, the pyridine could dissociate under mild conditions.²⁰

On the other hand, the chemistry of low valent middle or late transition metal alkylidyne/carbyne complexes has been well-established²¹ and some of these complexes exhibit remarkable stabilities toward air and moisture. [2 + 2] cycloaddition reactions of non- d^0 metal carbyne complexes with alkynes,^{22–25} olefins²⁶ or allenes²⁷ have been documented and a few

^aDepartment of Chemistry, The Hong Kong University of Science and Technology, Clear Water Bay, Kowloon, Hong Kong, P. R. China. E-mail: chjiag@ust.hk

^bHKUST Shenzhen Research Institute, 518057 Shenzhen, P. R. China

† Electronic supplementary information (ESI) available. CCDC 2360919, 2289258 and 2360920. For ESI and crystallographic data in CIF or other electronic format see DOI: <https://doi.org/10.1039/d4sc05369a>

‡ These authors contributed equally.

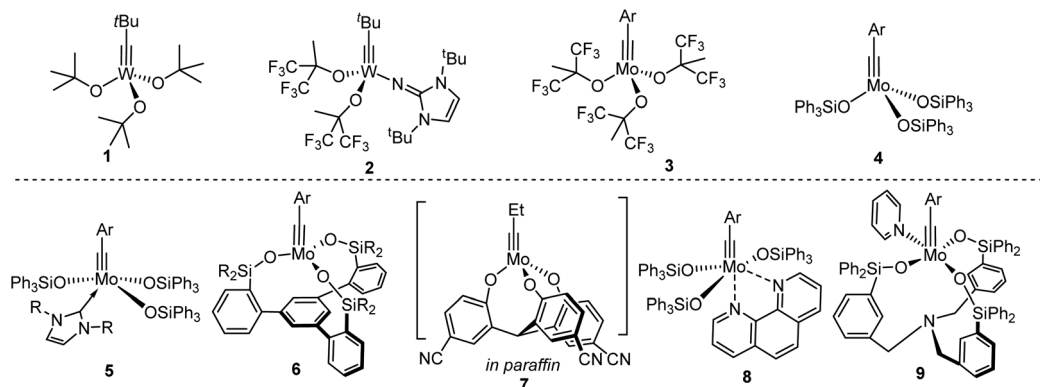


Chart 1 Selected structures of d^0 Mo/W alkylidyne complexes for alkyne metathesis.

stoichiometric alkyne metathesis reactions of $W(IV)^{28}$ and $Re(V)^{29}$ alkylidyne complexes have been observed, implying an alternative approach toward user-friendly alkyne metathesis catalysts. Indeed, our group recently reported a series of well-defined d^2 $Re(V)$ alkylidyne catalysts^{30–32} (e.g. **10a–c**, Scheme 1). These $Re(V)$ alkylidyne complexes, bearing two bulky phosphinophenolate (PO) ligands, induce the coordinated alkyne to align parallel to the alkylidyne ligand due to steric, thus facilitating $[2 + 2]$ cycloaddition.³³ These d^2 $Re(V)$ alkylidyne catalysts exhibit remarkable advantages such as stability in air, ease of handling, and excellent functional group compatibility. Despite these advantages, their catalytic activities are relatively low. They are inactive at ambient temperature and requires harsh conditions (100–110 °C) for activation, placing this series notably behind d^0 $Mo(VI)$ and $W(VI)$ alkylidyne catalysts in terms of efficiency. In this work, we report new $Re(V)$ alkylidyne-based catalysts that show significantly enhanced catalytic activity and can promote catalytic alkyne metathesis reactions at room temperature.

Results and discussion

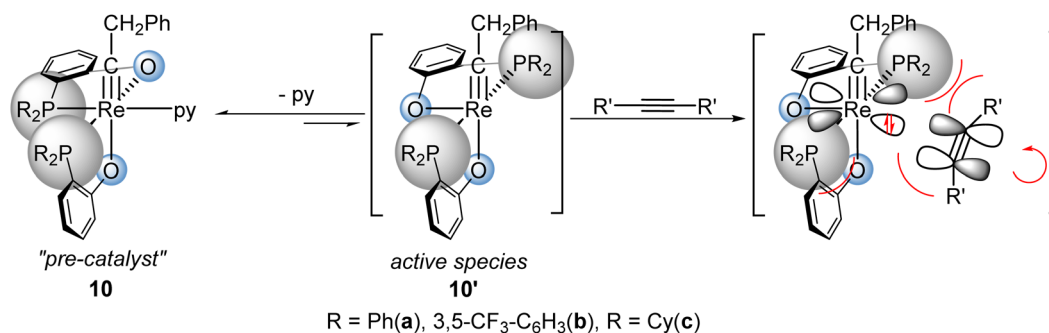
Synthesis of Re alkylidyne complexes

Alkyne metathesis reactions catalyzed by **10** involve initial dissociation of a pyridine ligand from **10** to form the 5-coordinated active species $Re(\equiv CCH_2Ph)(^RPO)_2$ (**10'**). The catalytic activity or the overall kinetic barrier of the catalytic reactions are expected to be influenced by both pyridine dissociation and the

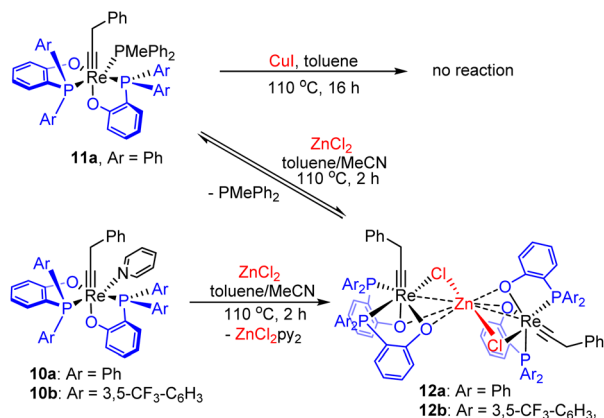
metathesis reaction of the active species $Re(\equiv CCH_2Ph)(^RPO)_2$ (**10'**). In this regard, it is appealing to isolate 5-coordinated complexes $Re(\equiv CR)(^RPO)_2$, which should be catalytically more active than the pyridine complexes **10**. In addition, the availability of such complexes will allow us to reveal the intrinsic barrier for metathesis reaction of active species $Re(\equiv CCH_2Ph)(^RPO)_2$ (**10'**).

Experimentally, we first attempted to isolate the 5-coordinated species $Re(\equiv CCH_2Ph)(^{Ph}PO)_2$ (**10a'**) from the readily available complex $Re(\equiv CCH_2Ph)(^{Ph}PO)_2(PMePh_2)$ (**11a**), which can be easily prepared in large scale from commercially available phosphine (see ESI†). Despite the fact that ligand substitution of **11a** with pyridine can be successfully achieved using CuI as a phosphine scavenger, yielding $Re(\equiv CCH_2Ph)(^{Ph}PO)_2(py)$ (**10a**), essentially no reaction occurred between the complex **11a** and CuI in the absence of pyridine. Therefore, a more efficient phosphine scavenger was sought.

Promising results were obtained with $ZnCl_2$. Heating a mixture of **11a** and anhydrous $ZnCl_2$ in a mixed solvent of toluene and acetonitrile ($v/v = 3:1$) at 110 °C for 2 hours, $PMePh_2$ dissociation occurred, together with the formation of the new Re alkylidyne complex **12a** (Scheme 2), as evidenced by the appearance of two broad singlet $^{31}P\{^1H\}$ signals at 37.6 and 26.2 ppm. However, attempts to isolate the complex failed as a result of the reaction with the released $PMePh_2$ to regenerate **11a** during workup. Interestingly, when a mixture of the pyridine complex **10a** and $ZnCl_2$ was heated, the same Re alkylidyne



Scheme 1 Examples of d^2 $Re(V)$ alkylidyne complexes serving as catalyst precursors for alkyne metathesis and the "bulky PO ligand strategy".



Scheme 2 Attempted extraction of PMePh_2 from $\text{Re}(\equiv\text{CCH}_2\text{-Ph})(^{\text{Ar}}\text{PO})_2(\text{PMePh}_2)$ with 3d transition metal salts.

complex **12a** was also produced (see Fig S4 and S5†). Similarly, the reaction of **10b** with ZnCl₂ produced analogous complex **12b**. It is the formation of stable ZnCl₂(pyridine)₂ adduct from the dissociated pyridine ligand and ZnCl₂ that prevents the reaction from reversing, enabling the isolation of complexes **12**. Pale yellow single crystals of **12b** were obtained, enabling the determination of its structure by single crystal X-ray diffraction.

The solid-state structure of **12b** reveals a confacial tri-octahedral Re-Zn-Re complex (Fig. 1). This structure can be

regarded as two $\text{Re}(\equiv\text{CCH}_2\text{Ph})(^{\text{Ar}}\text{PO})_2$ fragments stabilized by ZnCl_2 through chloride coordination. The $\text{Re}(1)\text{--Cl}(1)$ and $\text{Re}(2)\text{--Cl}(2)$ bond distances are 2.4798(13) Å and 2.5031(13) Å, respectively. The central Zn atom is 6-coordinated, with an average Zn–O bond length of 2.109 Å. The $\text{Zn}(1)\text{--Cl}(1)$ and $\text{Zn}(1)\text{--Cl}(2)$ bonds (2.4356(16) Å and 2.4377(16) Å) are significantly elongated from normal Zn–Cl bonds.³⁴ The chelating effect of phenolates together with a strong affinity of Zn for O, stabilize the ZnCl_2 bridge, allowing the isolation of **12**. However, it was found experimentally that the catalytic activity of **12a** in metathesis reactions is very low (entry 2, Table 1), consistent with the strong coordination of ZnCl_2 by the chelating oxygen ligands.

Taking a lesson from the formations of **12**, we searched for more efficient phosphine scavengers among coordinatively unsaturated 4d and 5d late transition metal complexes, as they possess a stronger affinity for phosphorous but a weaker affinity for oxygen. This may ensure efficient trapping of the PMePh₂ ligand without forming stable adducts with Re(v) alkylidyne, as observed in compounds **12**.

In dry toluene or benzene, complex **11a** reacted with one equivalent of $[(p\text{-cymene})\text{RuCl}_2]_2$, resulting in the formation of the expected complex $(p\text{-cymene})\text{RuCl}_2(\text{PMePh}_2)$ together with a rhenium alkylidyne complex. The latter exhibits two singlet $^{31}\text{P}\{^1\text{H}\}$ signals at 40.1 and 30.5 ppm, as well as characteristic doublets of triplets ^1H signals at 2.40 and 2.92 ppm for a $\text{Re}\equiv\text{CCH}_2$ group and four characteristic doublet ^1H signals of coordinated *p*-cymene (see Fig. S6 and S7† for details). Based on the NMR data and reactivity (see below), we tentatively assigned the new alkylidyne complex as the dinuclear complex **13**, wherein the $\text{Re}(\equiv\text{CCH}_2\text{Ph})(^{\text{ph}}\text{PO})_2$ fragment is stabilized by $(p\text{-cymene})\text{RuCl}_2$ through chloride coordination (Fig. 2).

Efforts to isolate pure complex **13** were unsuccessful due to its high moisture sensitivity. The species reacted readily with

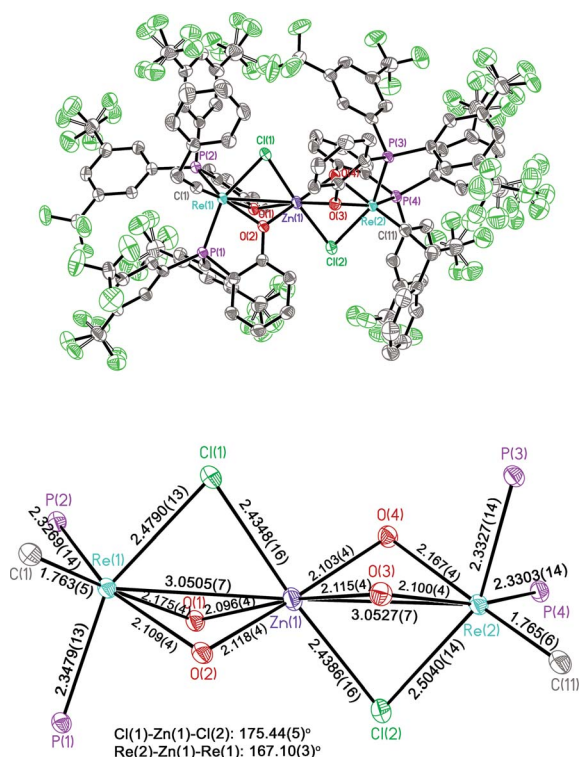
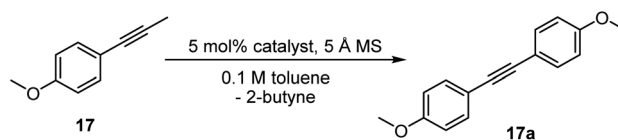


Fig. 1 Top: ORTEP diagram of the confacial trioctahedral complex **12b** with thermal ellipsoids at the 40% probability level. The solvent molecule as well as all hydrogen atoms are omitted for clarity. Bottom: selected bond lengths (Å) and angles (deg) of **12b**. Only the core atoms are shown for clarity.

Table 1 Catalytic performance of Re(v) alkylidynes^a

| Entry | Catalyst | <i>T</i> /°C | Time/h | Yield/% |
|-------|------------------------|--------------|--------|---------|
| 1 | 10a | 60 | 16 | Trace |
| 2 | 12a | 100 | 8 | 14 |
| 3 | 14 | 24 | 16 | 92 |
| 4 | 14 | 60 | 1 | >95 |
| 5 | 14 ^b | 60 | 3 | 84 |
| 6 | 15 | 24 | 16 | 85 |
| 7 | 16 | 60 | 16 | 58 |
| 8 | 15 | 24 | 1 | 95 |
| 9 | 16 | 60 | 1 | 92 |

^a Standard condition: 1-methoxy-4-(1-propyn-1-yl)benzene (**17**, 0.3 mmol), catalyst (5 mol%), 5 Å MS (450 mg), dry toluene (3 mL). The yields were determined by ¹H NMR using CH₂Ph₂ as an internal standard. ^b 0.5 mol% catalyst loading.



Fig. 2 (a) Synthesis of the aqua complex **14**. (b) Ligand substitution reactions of **14** with methyl thioether and 2-picoline. (c) Photograph of the aqua complex **14** stored under air atmosphere for 3 months.

a trace amount of water, yielding the aqua complex $\text{Re}(\equiv\text{CCH}_2\text{Ph})(^{\text{Ph}}\text{PO})_2(\text{H}_2\text{O})$ (**14**, Fig. 2). After allowing an NMR tube containing **13** to stand at room temperature overnight, yellow crystals of the aqua complex **14** deposited on the wall due to the involvement of trace moisture. Alternatively, gram-scale preparation of the aqua complex **14** can be achieved with a high yield by heating the complex **11a** with $[(p\text{-cymene})\text{RuCl}_2]_2$ and water in toluene. The pure product of **14** was obtained as an air and moisture stable yellow powder (Fig. 2c).

The structure of **14** has been confirmed by NMR, X-ray diffraction, and elemental analysis. As shown in Fig. 3, the complex adopts a distorted octahedral geometry bearing two *cis* PO ligands, similar to complexes **11a** and **10a**. The aqua ligand is *cis* to the alkylidyne ligand and *trans* to a phosphine. The $\text{Re}(1)\text{--P}(2)$ bond (*trans* to the $\text{Re}\text{--OH}_2$ bond) has a bond length of 2.3553(11) Å, which is shorter than the corresponding bonds in **11a** (2.3722(5) Å) and **10a** (2.4109(6) Å), implying that the *trans* influence of OH_2 is less than that of PMePh_2 and pyridine, hinting that the $\text{Re}\text{--OH}_2$ bond might be relatively weak. Consistent with the solid-state structure, the $^{31}\text{P}\{^1\text{H}\}$ NMR spectrum of **14** showed two singlets at 23.4 and 38.2 ppm; the ^1H NMR spectrum shows two multiplet signals at 2.65 and 1.32 ppm for the $\text{Re}\equiv\text{CCH}_2$ group and a singlet at 7.84 ppm for the bound H_2O . The compound **14** is only sparingly soluble in non-coordinating organic solvents such as benzene and dichloromethane, preventing the recording of the ^{13}C NMR spectrum.

The isolation of the aqua complex **14** confirms that $\text{Re}(\text{v})$ alkylidynes are indeed robust toward water. It's worth noting that structurally characterized aqua-alkylidyne complexes are

still rare.³⁵ The $\text{Re}(\text{vii})$ aqua alkylidyne complex $[\text{Re}(\equiv\text{C}-t\text{Bu})(\text{CH}_2-t\text{Bu})_3(\text{H}_2\text{O})]^+[\text{BAR}^{\text{F}}_4]^-$ has been previously reported by Schrock and his co-workers, although the structure of this complex was not confirmed by X-ray diffraction.³⁶

The isolation of the ZnCl_2 -bridged complexes **12**, the aqua complex **14** as well as the observation of the bimetallic complex **13** suggests that $\text{Re}(\text{v})$ alkylidynes bearing two PO ligands have a strong tendency to be 6-coordinated, even by incorporating a chloride salt or complex. As a result, attempts to isolate the 5-coordinated active species **10'** have been so far unsuccessful.

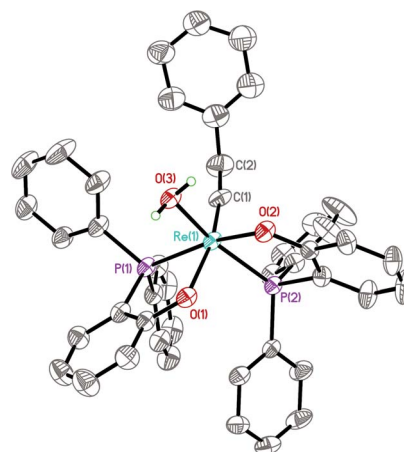


Fig. 3 ORTEP diagram of the aqua complex **14** with thermal ellipsoids at the 40% probability level. All hydrogen atoms except those of the water ligand are omitted for clarity. Selected bond lengths (Å) and angles (deg): $\text{Re}(1)\text{--C}(1)$ 1.759(5), $\text{Re}(1)\text{--O}(3)$ 2.173(3), $\text{Re}(1)\text{--P}(1)$ 2.3312(11), $\text{Re}(1)\text{--P}(2)$ 2.3553(11), $\text{O}(3)\text{--Re}(1)\text{--P}(2)$ 161.32(8).





Fig. 4 ORTEP diagram of the SMe_2 complex **15** with thermal ellipsoids at the 40% probability level. All hydrogen atoms as well as solvent atoms are omitted for clarity. Selected bond lengths (Å) and angles (deg): Re(O1)–C(1) 1.7690(18), Re(O1)–S(1) 2.4524(4), Re(O1)–P(1) 2.3370(4), Re(O1)–P(2) 2.3811(4), S(1)–Re(O1)–P(2) 164.018(15).

Echoing the weak Re–OH₂ bond indicated by the X-ray data, the aqua ligand of **14** is quite labile and can be easily substituted by other two-electron σ donors at room temperature. Utilizing this advantage, we can obtain other adducts of $\text{Re}(\equiv\text{CCH}_2\text{Ph})(^{\text{Ph}}\text{PO})_2$ that cannot be synthesized before. For instance, the SMe_2 adduct **15** could be quantitatively formed by treating the aqua complex **14** with 3 equivalents of methyl thioether at room temperature. Analogously, stirring a suspension of **14** with excess 2-picoline in toluene led to the quantitative formation of the 2-picoline complex **16**, which was isolated as a yellow solid in high yield (Fig. 2). Stirring **14** in O-donor solvents like ethers or acetone resulted in messy mixtures, and their structures remain unidentified.

New complexes **15** and **16** have been characterized by multinuclear NMR spectroscopy. The structure of the SMe_2 complex **15** has also been characterized by single crystal X-ray diffraction analysis (Fig. 4).

Benchmarking of alkyne metathesis

The lower affinity of OH₂ compared with pyridine and PMePh_2 for the Re(v) center suggests that the aqua complex **14** might be a more active alkyne metathesis catalyst than the phosphine complex **11a** and the pyridine complex **10a**. To compare the activity of the new complex **14** with those of the phosphine complex **11a** and the pyridine complex **10a**, we conducted kinetic studies on the model reaction, the homometathesis of 1-methoxy-4-(1-propyn-1-yl)benzene (**17**), catalyzed by 5 mol% complexes **14**, **11a** and **10a** at 100 °C, respectively, with 5 Å molecular sieves (MS) added as butyne scavenger.

The kinetic plots are presented in Fig. 5. Surprisingly, the aqua complex **14** exhibits significantly improved catalytic activity compared to **11a** and **10a** and the model reaction catalyzed by **14** was completed within 5 min (red line). In contrast, the reaction with the phosphine complex **11a** (olive line) and the pyridine complex **10a** (blue line) achieved conversions of less than 5% and ca. 50%, respectively, after 2 h.

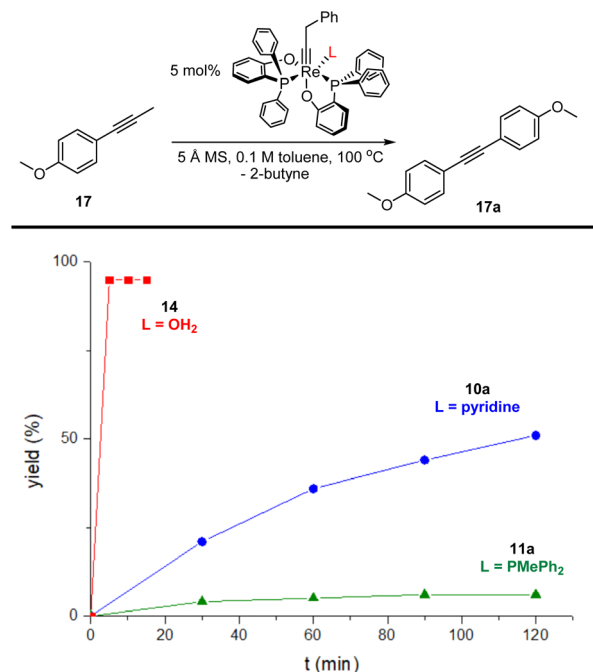


Fig. 5 Kinetic plots of homometathesis of 1-methoxy-4-(1-propyn-1-yl)benzene (**17**) mediated by catalysts **10a** (blue line), **11a** (olive line) and **14** (red line). Condition: substrate (**17**, 0.3 mmol), catalyst (5 mol%), 5 Å MS (450 mg), dry toluene (3 mL), 100 °C. The yields were determined by ¹H NMR using CH_2Ph_2 as an internal standard.

To our delight, the aqua complex **14** is catalytically active even at room temperature (Table 1, entry 3): The model reaction promoted by 5 mol% of aqua complex **14** proceeded to 92% conversion in 16 hours at room temperature (24 °C). This result is interesting as it represents the first demonstrated room temperature alkyne metathesis reaction catalyzed by a non-d⁰ alkylidyne complex. The activity of **14** increased significantly when slightly heated; the model reaction achieved full conversion within 1 hour at 60 °C (entry 4). With a loading of 0.5 mol% of the catalyst, the reaction at 60 °C achieved a conversion of 84% in 3 hours (entry 5), indicating that **14** is an catalyst with sufficiently high TON. The SMe_2 adduct **15** and the 2-picoline adduct **16** are also active at ambient temperature. The model reaction mediated by **15** and **16** yielded homometathesis product in 58% and 85% yields after 16 h at 24 °C. The results indicated that **15** and **16** are also efficient catalysts with activity similar to or slightly less than the aqua complex **14**.

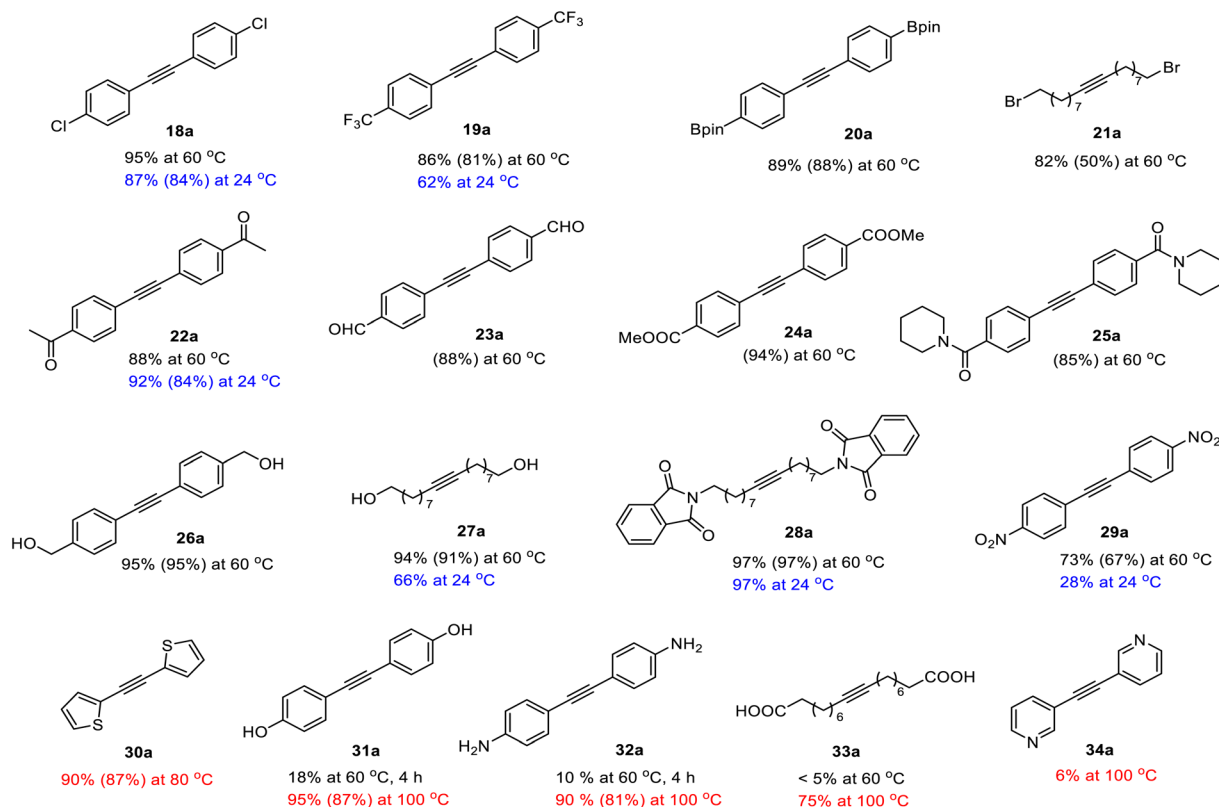
Substrate scope

To evaluate the functional group tolerance of the readily-available and user-friendly Re(v) catalyst **14**, we have investigated its capability in homometathesis reactions of a series of functionalized methyl-capped alkynes, as illustrated in Table 2. Metathesis reactions were typically carried out under an inert atmosphere with a 2 mol% catalyst loading. 5 Å molecular sieves (MS) were added as a 2-butyne abstractor to facilitate the reactions to go completion. The reactions were usually carried out at 60 °C. For some of the substrates, the reactions were also



$$2 \text{ R} \equiv \text{C} \xrightarrow[\text{- 2-butyne}]{\text{14 (2-5 mol\%), 5 \AA MS, toluene (0.1 M)}} \text{R} \equiv \text{C} - \text{C} \equiv \text{R}$$

18-34 **18a-34a**



^a Standard condition: substrate (0.3 mmol), catalyst (2–5 mol%), 5 Å MS (450 mg), dry toluene (3 mL). The yields were determined by ¹H NMR using CH₂Ph₂ as an internal standard. Isolated yields are given in parathesis. Reaction temperatures are color-labeled: blue: 24 °C, 16 h; black: 60 °C, 1–12 h; red: 80 °C or 100 °C, 4–16 h.

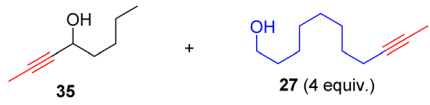
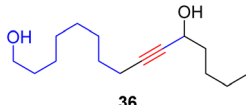
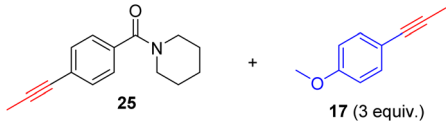
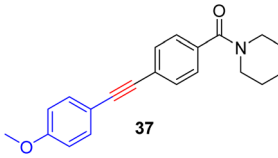
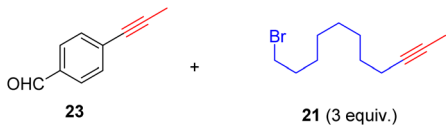
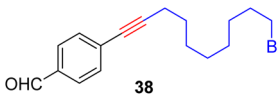
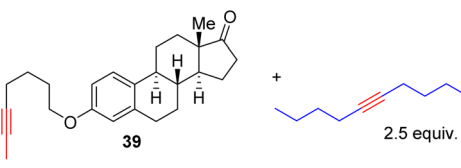
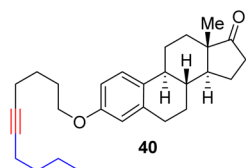
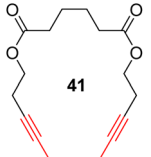
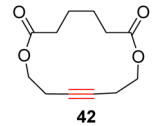
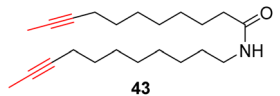
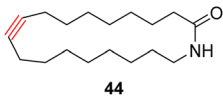
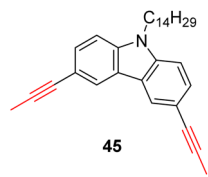
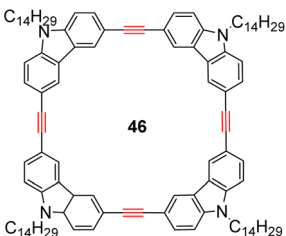
leading to slower reaction rates at ambient temperature. However, when the reaction was conducted at 60 °C, it proceeded more efficiently and achieved promising yield.

As previously mentioned, alkyne metathesis reactions mediated by **14** presumably proceed through alkyne-alkylidyne intermediates $\text{Re}(\equiv\text{CCH}_2\text{Ph})(\text{P}^{\text{Ph}}\text{O})_2(\eta^2\text{-alkyne})$ formed by displacement of the labile H_2O ligand in **14**. Consequently, the rates or kinetic barriers of alkyne metathesis reactions are closely related to or governed by the coordination ability of functional groups present in the substrates. Thus, reactions involving substrates with a weakly coordinating functional group (*e.g.*, Table 2, **18–28**) can achieve almost full conversion either at room temperature (24 °C) in 16 hours or at 60 °C within 1–8 hours. In contrast, substrates with a strongly coordinating functional group have reduced activity, due to competing coordination of the alkyne and the coordinating functional group. A higher temperature is required for such substrates to achieve a high conversion in a reasonably short period of time.

For example, the homometathesis of 2-thiophenyl-1-propyne (**30**) progressed slowly at 60 °C due to competing S coordination, but can complete at 80 °C within 8 hours to produce **30a** in 90% yield. As additional examples, homometathesis of 4-propynyl aniline (**32**) proceeded slowly at 60 °C (10% in 4 h) and requires a reaction temperature of 100 °C to go completion in 8 h, due to competing NH₂ coordination; homometathesis of the sterically unshielded pyridine substrate (**34**) yields only 6% of compound **34a** even after heating at 100 °C for 16 hours due to the coordination of pyridine. In contrast, sterically hindered amides, such as **25** and **28**, readily undergo metathesis, even at room temperature. Substrates with strong acidic functional groups also slow down metathesis reactions.

With the well-behaved alkyne metathesis catalyst **14** in hand, we have performed a series of representative alkyne metathesis reactions to show its applications in diverse scenarios (Table 3). The complex **14** is able to catalyze cross-metathesis (ACM) between two aliphatic alkynes (entries 1 and 4), two aromatic alkynes (entry 2), as well as an aliphatic and an aromatic alkynes (entry 3) to give crossed products in high yields. Entry 4 shows that the catalyst works well for a bio-active substrate, providing a new route to aliphatic alkyne modification. The catalyst also works well in ring-closing alkyne metathesis (RCAM) reactions, giving cyclic products in good to excellent yields (entries 5 and 6). The catalyst can also mediate acyclic diyne metathesis macrocyclization (ADIMAC). For example, the bispropynylated

Table 3 Representative alkyne metathesis reactions catalyzed by **14**^a

| Entry | Substrate (s) | Product | Yield ^b % |
|-------|-------------------------------------------------------------------------------------|---------------------------------------------------------------------------------------|----------------------|
| 1 |  |  | 67% |
| 2 |  |  | 69% |
| 3 |  |  | 61% |
| 4 |  |  | 72% |
| 5 |  |  | 92 ^c % |
| 6 |  |  | 68 ^d % |
| 7 |  |  | 98 ^e % |

^a Conditions: **14** (5 mol%), 5 Å MS, toluene, 60 °C, 1–4 h. ^b Isolated yields. ^c 80 °C, 8 h. ^d 100 °C, 12 h. ^e 60 °C, 14 h.



carbazole derivative **45** was efficiently converted to the macrocycle **46** (entry 7), demonstrating the potential usage of the catalytic system in constructing molecular rings and cages.

Conclusions

In this work, we have presented the first non- d^0 alkylidyne complex capable of effecting alkyne metathesis at room temperature, namely, the Re(v) alkylidyne complex $\text{Re}(\equiv\text{CCH}_2\text{Ph})(^{\text{Ph}}\text{PO})_2(\text{H}_2\text{O})$ (**14**), featuring a H_2O leaving ligand. Analogous complexes with labile ligands such as SMe_2 (**15**) and 2-picoline (**16**) also show remarkable activity in mediating alkyne metathesis at moderate temperatures. The d^2 Re(v)-alkylidyne catalysts now exhibits activity comparable with or approaching to those of d^0 Mo(vi)/W(vi) alkylidyne catalytic systems. This study also implies that the impact of metal d electrons on the kinetic barrier of $[2 + 2]$ cycloaddition of a non- d^0 alkylidyne and an alkyne can be significantly diminished by employing suitable ligands.

The aqua complex **14** is stable to air and moisture in the solid state, enabling storage and handling in air. It can efficiently promote alkyne homometathesis, cross-metathesis (ACM), ring-closing alkyne metathesis (RCAM), as well as acyclic diyne metathesis macrocyclization (ADIMAC) reactions, and tolerate a broad range of functional groups. Last but not least, the complex **14** can be readily prepared on a large scale from commercially available starting materials. Thus it represents a practical alkyne metathesis catalytic system based on d^2 Re(v)-alkylidynes.

Data availability

Crystallographic data for **12b**· 2CHCl_3 (CCDC no. 2360919), **14**· $0.5\text{C}_7\text{H}_8$ (CCDC no. 2289258), and **15** (CCDC no. 2360920) have been deposited at The Cambridge Crystallographic Data Centre via <https://www.ccdc.cam.ac.uk/structures/>.

Author contributions

G. J. and M. C. conceived the project. M. C. and J. H. performed synthetic experiments. L. Y. T. contributed to scope studies. H. H. Y. S. and I. D. W. collected and refined the X-ray data. M. C. and G. J. wrote the manuscript. G. J. supervised the project. All authors have given approval to the final version of the manuscript.

Conflicts of interest

The authors declare the following competing financial interest: A provisional patent application has been filed.

Acknowledgements

This work was supported by the National Natural Science Foundation of China (project no.: 21971218) and the Hong Kong Research Grants Council (project no.: 16308721, 16302322).

Notes and references

- Selected reviews:(a) M. Cui and G. Jia, *J. Am. Chem. Soc.*, 2022, **144**, 12546; (b) A. Fürstner, *J. Am. Chem. Soc.*, 2021, **143**, 15538; (c) D. Lee, I. Volchkov and S. Y. Yun, *Org. React.*, 2020, **102**, 613; (d) H. Ehrhorn and M. Tamm, *Chem.-Eur. J.*, 2019, **25**, 3190; (e) R. R. Schrock, *Chem. Commun.*, 2013, **49**, 5529.
- Recent examples:(a) J. L. Sutro and A. Fürstner, *J. Am. Chem. Soc.*, 2024, **146**, 2345; (b) T. Varlet, S. Portmann and A. Fürstner, *J. Am. Chem. Soc.*, 2023, **145**, 21197; (c) J. Tang, W. Li, T. Y. Chiu, F. Martinez-Pena, Z. Luo, C. T. Chong, Q. Wei, N. Gazaniga, T. J. West, Y. Y. See, L. L. Lairson, C. G. Parker and P. S. Baran, *Nature*, 2023, **622**, 507; (d) Z. Meng, S. M. Spohr, S. Tobegen, C. Farès and A. Fürstner, *J. Am. Chem. Soc.*, 2021, **143**, 14402; (e) E. Yiannakas, M. I. Grimes, J. T. Whitelegge, A. Fürstner and A. N. Hulme, *Angew. Chem., Int. Ed.*, 2021, **60**, 18504; (f) A. G. Dalling, G. Späth and A. Fürstner, *Angew. Chem., Int. Ed.*, 2022, **61**, e202209651.
- Selected reviews on diyne metathesis polymerization:(a) H. Yang, Y. Jin, Y. Du and W. Zhang, *J. Mater. Chem. A*, 2014, **2**, 5986; (b) U. H. F. Bunz, *Acc. Chem. Res.*, 2001, **34**, 998; (c) M. Ortiz, C. Yu, Y. Jin and W. Zhang, *Top. Curr. Chem.*, 2017, **375**, 69.
- Selected examples of ring-opening alkyne metathesis polymerization: (a) S. von Kugelgen, R. Sifri, D. Bellone and F. R. Fischer, *J. Am. Chem. Soc.*, 2017, **139**, 7577; (b) S. von Kugelgen, I. Piskun, J. H. Griffin, C. T. Eckdahl, N. N. Jarenwattananon and F. R. Fischer, *J. Am. Chem. Soc.*, 2019, **141**, 11050.
- H. Jeong, S. von Kugelgen, D. Bellone and F. R. Fischer, *J. Am. Chem. Soc.*, 2017, **139**, 15509.
- Selected examples of acyclic diyne metathesis macrocyclization:(a) S. Huang, Z. Lei, Y. Jin and W. Zhang, *Chem. Sci.*, 2021, **12**, 9591; (b) Y. Hu, C. Wu, Q. Pan, Y. Jinx, R. Lyu, V. Martinez, S. Huang, J. Wu, L. J. Wayment, N. A. Clark, M. B. Raschke, Y. Zhao and W. Zhang, *Nat. Synth.*, 2022, **1**, 449; (c) A. J. Greenlee, H. Chen, C. I. Wendell and J. S. Moore, *J. Org. Chem.*, 2022, **87**, 8429; (d) G. R. Kiel, K. L. Bay, A. E. Samkian, N. J. Schuster, J. B. Lin, R. C. Handford, C. Nuckolls, K. N. Houk and T. D. Tilley, *J. Am. Chem. Soc.*, 2020, **142**, 11084; (e) X. Jiang, J. D. Laffoon, D. Chen, S. Perez-Estrada, A. S. Danis, J. Rodriguez-Lopez, M. A. Garcia-Garibay, J. Zhu and J. S. Moore, *J. Am. Chem. Soc.*, 2020, **142**, 6493.
- Z. Lei, H. Chen, S. Huang, L. J. Wayment, Q. Xu and W. Zhang, *Chem. Rev.*, 2024, **124**, 7829.
- Selected pioneering works:(a) L. G. McCullough and R. R. Schrock, *J. Am. Chem. Soc.*, 1984, **106**, 4067; (b) L. McCullough, R. Schrock, J. Dewan and J. Murdzek, *J. Am. Chem. Soc.*, 1985, **107**, 5987.
- (a) J. Heppekaussen, R. Stade, R. Goddard and A. Fürstner, *J. Am. Chem. Soc.*, 2010, **132**, 11045; (b) J. Heppekaussen, R. Stade, A. Kondoh, G. Seidel, R. Goddard and A. Fürstner, *Chem.-Eur. J.*, 2012, **18**, 10281.



- 10 Selected pioneering works:(a) J. H. Wengrovius, J. Sancho and R. R. Schrock, *J. Am. Chem. Soc.*, 1981, **103**, 3932; (b) M. R. Churchill, J. W. Ziller, J. H. Freudenberger and R. R. Schrock, *Organometallics*, 1984, **3**, 1554; (c) J. H. Freudenberger, R. R. Schrock, M. R. Churchill, A. L. Rheingold and J. W. Ziller, *Organometallics*, 1984, **3**, 1563; (d) S. Beer, C. G. Hrib, P. G. Jones, K. Brandhorst, J. Grunenberg and M. Tamm, *Angew. Chem., Int. Ed.*, 2007, **46**, 8890; (e) S. Lysenko, J. Volbeda, P. G. Jones and M. Tamm, *Angew. Chem., Int. Ed.*, 2012, **51**, 6757.
- 11 U. H. F. Bunz, *Science*, 2005, **308**, 216.
- 12 (a) Y. Ge, Y. Hu, G. Duan, Y. Jin and W. Zhang, *Trends Chem.*, 2022, **4**, 540; (b) K. Jyothish and W. Zhang, *Angew. Chem., Int. Ed.*, 2011, **50**, 8478.
- 13 (a) J. V. Musso, V. Gramm, S. Stein, W. Frey and M. R. Buchmeiser, *Eur. J. Inorg. Chem.*, 2022, **26**, e202200649; (b) J. Groos, P. M. Hauser, M. Koy, W. Frey and M. R. Buchmeiser, *Organometallics*, 2021, **40**, 1178; (c) I. Elser, J. Groos, P. M. Hauser, M. Koy, M. van der Ende, D. R. Wang, W. Frey, K. Wurst, J. Meisner, F. Ziegler, J. Kastner and M. R. Buchmeiser, *Organometallics*, 2019, **38**, 4133; (d) M. Koy, I. Elser, J. Meisner, W. Frey, K. Wurst, J. Kastner and M. R. Buchmeiser, *Chem.-Eur. J.*, 2017, **23**, 15484.
- 14 (a) J. Hillenbrand, M. Leutzsch, E. Yiannakas, C. P. Gordon, C. Wille, N. Nöthling, C. Copéret and A. Fürstner, *J. Am. Chem. Soc.*, 2020, **142**, 11279; (b) J. Hillenbrand, M. Leutzsch and A. Fürstner, *Angew. Chem., Int. Ed.*, 2019, **58**, 15690.
- 15 (a) R. R. Thompson, M. E. Rotella, X. Zhou, F. R. Fronczek, O. Gutierrez and S. Lee, *J. Am. Chem. Soc.*, 2021, **143**, 9026; (b) R. R. Thompson, M. E. Rotella, P. Du, X. Zhou, F. R. Fronczek, R. Kumar, O. Gutierrez and S. Lee, *Organometallics*, 2019, **38**, 4054.
- 16 Other examples with a tripodal ligand:(a) J. Hillenbrand, M. Leutzsch, C. P. Gordon, C. Copéret and A. Fürstner, *Angew. Chem., Int. Ed.*, 2020, **59**, 21758; (b) S. Schaubach, K. Gebauer, F. Ungeheuer, L. Hoffmeister, M. K. Ilg, C. Wirtz and A. Fürstner, *Chem. - Eur. J.*, 2016, **22**, 8494.
- 17 Y. Ge, S. Huang, Y. Hu, L. Zhang, L. He, S. Krajewski, M. Ortiz, Y. Jin and W. Zhang, *Nat. Commun.*, 2021, **12**, 1136.
- 18 (a) Y. Du, H. Yang, C. Zhu, M. Ortiz, K. D. Okochi, R. Shoemaker, Y. Jin and W. Zhang, *Chem.-Eur. J.*, 2016, **22**, 7959; (b) H. Yang, Z. Liu and W. Zhang, *Adv. Synth. Catal.*, 2013, **355**, 885; (c) K. Jyothish, Q. Wang and W. Zhang, *Adv. Synth. Catal.*, 2012, **354**, 2073; (d) K. Jyothish and W. Zhang, *Angew. Chem., Int. Ed.*, 2011, **50**, 3435.
- 19 M. Bindl, R. Stade, E. K. Heilmann, A. Picot, R. Goddard and A. Fürstner, *J. Am. Chem. Soc.*, 2009, **131**, 9468.
- 20 J. N. Korber, C. Wille, M. Leutzsch and A. Fürstner, *J. Am. Chem. Soc.*, 2023, **145**, 26993.
- 21 Selected reviews see:(a) H. P. Kim and R. J. Angelici, *Adv. Organomet. Chem.*, 1987, **27**, 51; (b) A. Mayr and H. Hoffmeister, *Adv. Organomet. Chem.*, 1991, **32**, 227; (c) P. F. Engel and M. Pfeffer, *Chem. Rev.*, 1995, **95**, 2281; (d) M. A. Esteruelas, A. M. López and M. Oliván, *Coord. Chem. Rev.*, 2007, **251**, 795; (e) G. Jia, *Coord. Chem. Rev.*, 2007, **251**, 2167; (f) T. Bolaño, M. A. Esteruelas and E. Oñate, *J. Organomet. Chem.*, 2011, **696**, 3911; (g) C. Shi and G. Jia, *Coord. Chem. Rev.*, 2013, **257**, 666; (h) R. A. Manzano and A. F. Hill, *Adv. Organomet. Chem.*, 2019, **72**, 103.
- 22 (a) C. Zhu, J. Zhu, X. Zhou, Q. Zhu, Y. Yang, T. B. Wen and H. Xia, *Angew. Chem., Int. Ed.*, 2018, **57**, 3154; (b) Z. Lu, Y. Cai, Y. Wei, Q. Lin, J. Chen, X. He, S. Li, W. Wu and H. Xia, *Polym. Chem.*, 2018, **9**, 2092; (c) Z. Lu, C. Zhu, Y. Cai, J. Zhu, Y. Hua, Z. Chen, J. Chen and H. Xia, *Chem.-Eur. J.*, 2017, **23**, 6426; (d) C. Zhu, Y. Yang, M. Luo, C. Yang, J. Wu, L. Chen, G. Liu, T. Wen, J. Zhu and H. Xia, *Angew. Chem., Int. Ed.*, 2015, **54**, 6181.
- 23 U. Das, PhD thesis, University of Bonn Mensch & Buch Verlag, Berlin, ISBN: 978-3-86387-551-0, 2014.
- 24 H. Fischer and C. Troll, *J. Chem. Soc. Chem. Commun.*, 1994, 457.
- 25 A. Mayr, K. S. Lee and B. Kahr, *Angew. Chem., Int. Ed.*, 1988, **27**, 1730.
- 26 M. A. Esteruelas, A. I. González, A. M. López and E. Oñate, *Organometallics*, 2004, **23**, 4858.
- 27 J. Rao, S. Dong, C. Yang, Q. Liu, X. Leng, D. Wang, J. Zhu and L. Deng, *J. Am. Chem. Soc.*, 2023, **145**, 25766.
- 28 (a) L. M. Atagi, S. C. Critchlow and J. M. Mayer, *J. Am. Chem. Soc.*, 1992, **114**, 9223; (b) L. M. Atagi and J. M. Mayer, *Organometallics*, 1994, **13**, 4794.
- 29 (a) W. Bai, K.-H. Lee, H. H. Y. Sung, I. D. Williams, Z. Lin and G. Jia, *Organometallics*, 2016, **35**, 3808; (b) W. Bai, W. Wei, H. H. Y. Sung, I. D. Williams, Z. Lin and G. Jia, *Organometallics*, 2018, **37**, 559.
- 30 M. Cui, H. H. Y. Sung, I. D. Williams and G. Jia, *J. Am. Chem. Soc.*, 2022, **144**, 6349.
- 31 M. Cui, W. Bai, H. H. Y. Sung, I. D. Williams and G. Jia, *J. Am. Chem. Soc.*, 2020, **142**, 13339.
- 32 L. Y. Tsang, W. Bai, L. C. Kong, H. H. Y. Sung, I. D. Williams and G. Jia, *Organometallics*, 2024, **43**, 849.
- 33 For computational studies, see: M. Tomasini, M. Gimferrer, L. Caporaso and A. Poater, *Inorg. Chem.*, 2024, **63**, 5842.
- 34 (a) J. Qin, N. Su, C. Dai, C. Yang, D. Liu, M. W. Day, B. Wu and C. Chen, *Polyhedron*, 1999, **18**, 3461; (b) C. de Cires-Mejias, S. Tanase, J. Reedijk, F. González-Vílchez, R. Vilaplana, A. M. Mills, H. Kooijman and A. L. Spek, *Inorg. Chim. Acta*, 2004, **357**, 1494; (c) A. D. Finke, D. L. Gray and J. S. Moore, *Acta Crystallogr., Sect. E: Crystallogr. Commun.*, 2016, **72**, 35.
- 35 Examples see: (a) W. Bai, K.-H. Lee, W. Y. Hung, H. H. Y. Sung, I. D. Williams, Z. Lin and G. Jia, *Organometallics*, 2017, **36**, 657; (b) W.-M. Xue, M. C. W. Chan, T. C. W. Mak and C.-M. Che, *Inorg. Chem.*, 1997, **36**, 6437; (c) W.-M. Xue, Y. Wang, T. C. W. Mak and C.-M. Che, *J. Chem. Soc., Dalton Trans.*, 1996, 2827.
- 36 A. M. LaPointe and R. R. Schrock, *Organometallics*, 1995, **14**, 1875.

